Small Angle Polarized Neutrons (SANSPOL) Investigation of Surfactant Free Magnetic Fluid of Uncoated and Silica-Coated Cobalt−Ferrite Nanoparticles

Massimo Bonini,[†] Albrecht Wiedenmann,[‡] and Piero Baglioni*[,†]

Department of Chemistry and CSGI, University of Florence, via della Lastruccia 3, I-50019 Sesto Fiorentino (Florence), Italy, and Hahn-Meitner-Institut, Glienicker Strasse 100, D-14109 Berlin, Germany

Received: February 17, 2004; In Final Form: May 9, 2004

Magnetic fluids formed from uncoated and silica-coated cobalt−ferrite nanoparticles dispersed in water have been synthesized and characterized by means of transmission electron microscopy (TEM) and small angle neutron scattering of polarized neutrons (SANSPOL). Particle shape, size, size distribution of the cores, and shell thickness, as obtained from the above-mentioned techniques, are reported for both uncoated and silica-coated cobalt−ferrite nanoparticles. SANSPOL takes advantage of the modification of contrast for the two magnetic polarization states, making possible the separation from the scattering of the magnetic and nonmagnetic contributions of the nanoparticles, and allowing a complete characterization of magnetic and diamagnetic domains of nanoparticles. The superiority of the SANSPOL technique over TEM is highlighted.

Introduction

Ferrofluids are stable colloidal suspensions of magnetic nanoparticles dispersed in a liquid. Since their first appearance in the middle of the 1960s,[1] interest in magnetic fluids has constantly grown, mainly because of their potential large number of applications in different fields such as magnetism, optics, rheology, biophysics, medicine, and thermodynamics.[2]

Many synthetic methodologies have been used to produce magnetic nanoparticles and to improve their properties. The most relevant synthetic pathways are the mechanical alloying processes (grinding, ball-milling, etc.), the use of nanoreactors as microemulsions, and the synthesis from supersaturated solutions. In particular, synthesis in nanoreactors appears today as one of the most powerful techniques to obtain monodisperse metallic nanoparticles with a good control of particle shape.[3−5] Unfortunately, only diluted dispersions (with a small amount of solid material content) can be obtained from this route. This makes the microemulsion technique attractive only for very demanding applications, due to the high production costs.

In the past twenty years, particular interest has been devoted to the ferrofluids synthesized by Massart's method,[6] i.e., dispersions in water of ultrasmall magnetic nanoparticles ($d \leq$ 15 nm), stabilized by an appropriate particle surface treatment. Due to the easy and economic preparation methodology, these magnetic fluids are ideal for several technological applications, especially when production costs are prominent to performance. However, pure magnetic nanoparticles themselves may not be very useful in practical applications because of the possible degradation when they are directly exposed to oxygen, resulting in the alteration of their magnetic properties. Ferrofluids prepared from Massart's methodology are considerably affected by these problems since the electric layer stabilizing the dispersion is "weaker", from the point of view of chemical and physical stabilization, than a layer constituted by surfactant molecules adsorbed at the surface of nanoparticles. In addition, magnetic fluids have the tendency to form aggregates. Various size sorting techniques are under development, but until now the results do not seem to be as good as the particle synthesis in microemulsions.[7,8] Magnetic fluids do not need to be completely monodisperse for a consistent number of industrial applications, although they need to be chemically and physically stable. It has been previously shown[9,10] that the presence of a shell of an inert material such as silica on the surface of ferrite nanoparticles prevents their aggregation and protects the magnetic particles from possible decomposition induced by the surrounding environment and in particular by oxygen. Moreover, the silica surface chemistry is well established, and silica-coated nanoparticles can be easily functionalized, making them biocompatible. In fact, the presence of silanol groups allows reaction with various coupling agents,[11−13] opening the use of these nanoparticle systems to a large number of applications.

Characterization of ferrofluids is not always easy. In particular, the evaluation of the size distribution of a dispersion of core−shell nanoparticles can be a very demanding task. Considering the incompleteness of the statistic, microscopy techniques such as transmission electron microscopy cannot give a full picture of the system under investigation, especially for core−shell nanoparticles. For these systems it is not always simple to distinguish between the inner and the outer part of the nanoparticles, especially when the electronic contrasts between the core and the shell are similar, or when the thickness of the coating shell or the diameter of the core are very small.

Scattering techniques are not affected by statistical problems. In particular, the size and size distribution of dispersions of very small nanoparticles can be obtained from small angle neutron and X-ray scattering by fitting the intensity of the scattered curves. However, the extraction of structural information from scattering data can be difficult when the contrast (i.e., scattering length density) of the core and of the nanoparticle shell are similar. This is the case of ferrites and silica-coated nanoparticles. It has been shown that[14−18] using polarized neutrons the relative contrasts for small-angle scattering of magnetic systems are strongly modified. In this paper, we used this property to

* Corresponding author. Phone: +39-055-457-3033 Fax: +39-055-457-3032. E-mail: baglioni@csgi.unifi.it. Internet: http://www.csgi.unifi.it.
[†] University of Florence.
[‡] Hahn-Meitner-Institut.

10.1021/jp049286a CCC: $27.50
Published on Web 09/02/2004

TABLE 1: Solutions Used to Prepare Magnetic Fluids[a]

solution	salt dissolved	amount	final volume	concentration
A	$FeCl_3 \cdot 6H_2O$	4.32 g	16 mL	1 M
B	$Co(NO_3)_2 \cdot 6H_2O$	2.33 g	8 mL	1 M
C	NaOH	4.00 g	100 mL	1 M
D	$Fe(NO_3)_3 \cdot 9H_2O$	2.83 g	14 mL	0.5 M
E	$Co(NO_3)_2 \cdot 6H_2O$	1.02 g	7 mL	0.5 M

[a] In the last column the concentrations of the metallic ions in solutions are reported. Water was degassed by bubbling nitrogen for 30 min before preparing solutions. In the same way, solutions were kept under a nitrogen flux before their use.

evaluate the magnetic composition of core−shell nanoparticles and we compared the results to transmission electron microscopy. The analysis of small angle data of polarized neutrons allows a complete description of the size, size distribution, layer thickness, and magnetic composition of the uncoated and silica-coated cobalt−ferrite nanoparticles.

Experimental Section

Reagents. Iron(II) chloride hexahydrate (97%) and tetraethyl ortho-silicate (>90%) were purchased from Aldrich. Sodium hydroxide (99%), cobalt(II) nitrate hexahydrate (99%), concentrated nitric acid (90%), iron(III) nitrate nonahydrate (>98%), and acetone (99.5%) were purchased from Fluka. 2-Propanol (99.7%) was purchased from Merck. Ammonium hydroxide water solution (puriss. 30−33wt %) was purchased from Riedel de Haen. Deuterated water (99.90%) was purchased from Euriso-top. All reagents were used as received.

Synthesis of Magnetic Fluids. *Uncoated Cobalt−Ferrite Nanoparticles.* Ferrofluids were synthesized using minor modifications of Massart's method.[6] Five solutions were prepared (see Table 1). Solutions A and B were added to concentrated nitric acid. In this synthetic step, the $Fe^{3+}-Co^{2+}$ mixture is kept in an acidic medium in order to avoid a possible metal hydrolysis before the base addition. This mixture and solution C were separately warmed to the boiling point and then mixed together as fast as possible under vigorous agitation. The boiling temperature and the agitation were maintained for at least 2 h. The precipitate was separated from the supernatant by magnetic decantation and washed with water. The precipitate was again separated by magnetic decantation and dispersed in a 2 M HNO_3 solution. This mixture was kept under vigorous agitation for 30 min; the precipitate was isolated again by magnetic decantation, and then dispersed during 1 h in a mixture of solutions D and E, already at the boiling temperature. The precipitate obtained after this treatment was isolated, washed once with a 1 M HNO_3 solution and twice with acetone, and then dispersed in 5 mL of water. The water dispersion was then kept in moderated vacuum at 40 °C in order to eliminate the residual acetone. The ferrofluid was then centrifuged at 4500 g for 5 min and the precipitate was discarded. Throughout the paper, we will indicate this nanoparticle dispersion as *un-FF* (*un*-coated *F*erro*F*luid).

Coated Cobalt−Ferrite Nanoparticles. The silica shell on the cobalt−ferrite nanoparticles was synthesized according to the following procedure.[12,19] An aliquot (0.3 mL) of the uncoated nanoparticles, prepared as described in the above paragraph, was added at room temperature to 4 mL of water and 20 mL of 2-propanol. Under stirring, 0.5 mL of ammonia water solution (30−33 wt %) and 100 μL of TEOS were consecutively added. This procedure was repeated every 20 min for a number of times so that the final thickness of the shell was 2 nm (in the hypothesis that all the nanoparticles would be covered by a uniform coating). The core−shell nanoparticles were separated from the reaction medium by centrifuging at 4500 g for 30 min and then dispersed in water. To take advantage of the variation of contrasts between the particles and the solvent, a second silica-coated nanoparticle batch was synthesized in a H_2O/D_2O 30/70% vol. mixture. Throughout the paper, we will indicate these ferrofluids as *co-FF* (*co*ated *F*erro*F*luids).

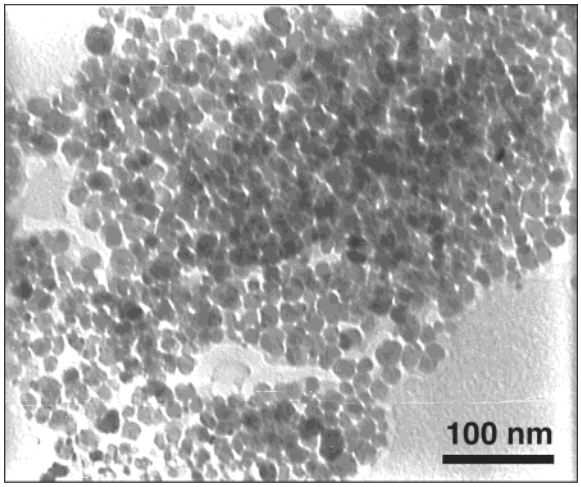

Figure 1. TEM micrograph of the uncoated cobalt−ferrite ferrofluid.

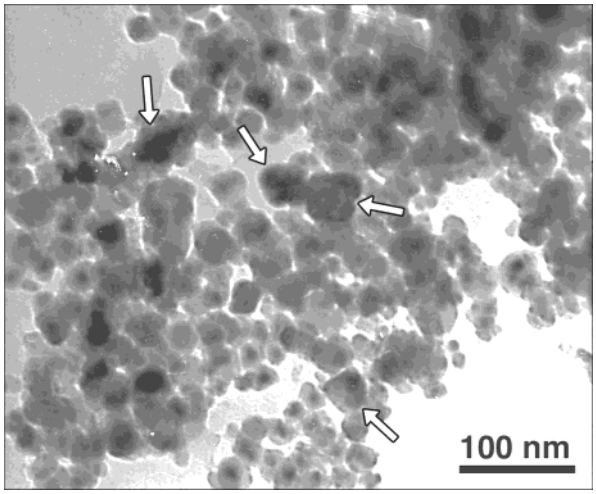

Figure 2. TEM micrograph of the silica-coated cobalt−ferrite ferrofluid. Arrows indicate bigger particles apparently constituted by clusters of cobalt−ferrite nanoparticles, held together by the silica coating.

TEM Measurements. Transmission electron microscopy investigations have been carried out using a Philips EM201C apparatus operating at 80 kV. Measurements were performed on both uncoated and silica-coated cobalt−ferrite nanoparticles. To easily evaluate dimensions of the particles, aliquots of the magnetic fluids were diluted in water in a 1:100 ratio. Samples were prepared by placing a 20 μL drop of these diluted magnetic fluids onto a carbon-coated copper grid. During the depositions the TEM grids were placed on a filter paper and were dried in a nitrogen atmosphere overnight. To obtain a good statistic, the diameters of more than three hundred nanoparticles for each sample have been measured.

SANSPOL. Small angle neutron scattering measurements of polarized neutrons were performed with the V4 instrument at the BERII reactor of the Hanh Meitner Institute, Berlin.[15] A horizontal magnetic field strength up to 1.1 T was applied at the sample position, oriented perpendicularly to the incoming neutrons. Polarized neutrons are provided by a transmission polarizing super-mirror cavity. The polarization direction is reversed using a spin flipper in front of the sample.

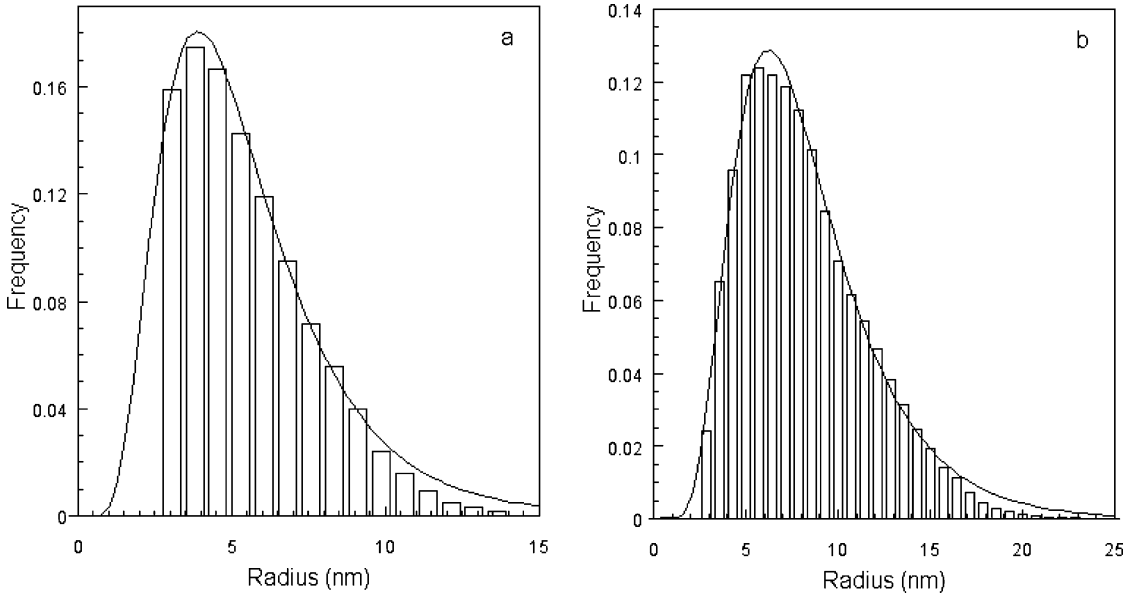

Figure 3. Size distribution of the un-FF (a) and co-FF (b), as obtained from the analysis of TEM micrographs. The histogram in figure b reports the external radius of the nanoparticles (i.e., core + shell radius). The solid lines represent the best fits of the data according to a log-normal distribution. The areas of the size distributions have been normalized to one.

For polarized neutrons, where the neutron spins are aligned antiparallel (+) or parallel (−) to the magnetic field vector *H*, the scattering cross-sections depend on the polarization *P* of the incident neutrons $I^+(Q)$ and $I^-(Q)$, respectively.[14] The scattering intensity (denoted here as SANSPOL) has been previously derived[16,20] and depends on the polarization state according to the following equations:

$$I^+(Q,\alpha) = A(Q) + B^+(Q)\sin^2\alpha \quad (1)$$

$$I^-(Q,\alpha) = A(Q) + B^-(Q)\sin^2\alpha \quad (2)$$

where α is the azimuth angle between the vectors H and Q, while *A*(Q) and *B*(Q) are the isotropic and anisotropic terms, respectively.

The arithmetic mean of the intensities corresponds to the intensity of a nonpolarized beam (denoted here as SANS):

$$[I^+(Q,\alpha) + I^-(Q,\alpha)]/2 = I(Q,\alpha)_{\text{non-polarized}} = A(Q) + B(Q)\sin^2\alpha \quad (3)$$

In the case of a dilute system of noninteracting particles, for complete alignment of all moments along the external field, the isotropic term is constituted only by the nuclear contribution $A(Q) = F_N^2$. As a consequence, both the SANS and the SANSPOL intensity parallel to H are independent of the polarization state resulting from pure nuclear contrast and given by

$$I(Q\|H) = A(Q) = F_N^2 \quad (4)$$

Considering again the case of a dilute system of noninteracting particles with all the moments aligned along H, the SANS intensity perpendicular to the applied field is given by

$$I(Q\perp H) = F_N^2 + F_M^2 \quad (5)$$

while the SANSPOL intensities perpendicular to the applied field are given for the two states by

$$I^{(-,+)}(Q\perp H) = [F_N \pm F_M]^2 \quad (6)$$

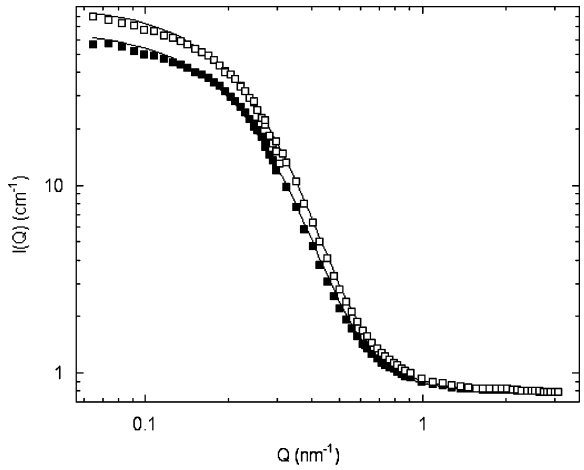

Figure 4. SANSPOL intensities perpendicular to the applied field of un-FF: $I^+(Q\perp H)$ (■) and $I^-(Q\perp H)$ (□). Solid lines represent the best fittings according to a spherical model.

This last equation explains the usefulness of the SANSPOL technique in separating weak magnetic contributions from strong nuclear contributions to the scattering intensity.

Results and Discussion

TEM Analysis. TEM pictures were collected for both uncoated and silica-coated cobalt−ferrite nanoparticle dispersions prepared as described in the Experimental section. Figures 1 and 2 show two representative images of the un-FF and the co-FF samples, respectively. In Figure 3a and 3b the size distributions obtained for the same sample from TEM images analysis are reported. The size distributions reported throughout this paper have been normalized by imposing the area of the distribution equal to 1.

TEM pictures show that un-FF particles are quite polydisperse and the shape is almost spherical, in agreement with previous results.[8,21−23] It is also clear from the analysis of TEM images that for co-FF the evaluation of the thickness of the silica shell is quite difficult. In fact, while the measurement of the external diameter does not constitute a problem, the border between the core and the shell of the particles is not clearly detectable due

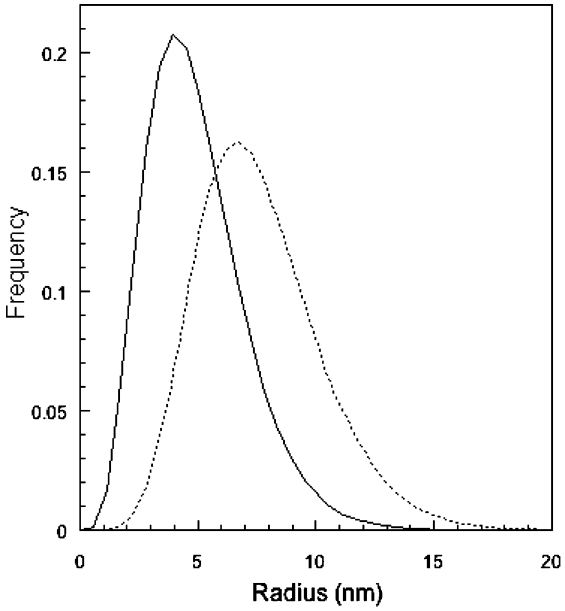

Figure 5. Size distribution (solid line) and volume weighted size distribution (dotted line) extracted from the fitting of un-FF SANSPOL experimental data.

to the poor "optical" contrast. For this reason, in Figure 3b we reported only the external diameter of the nanoparticles.

A comparison of the TEM micrographs evidences that co-FF presents larger particles than un-FF. Moreover, while the coated nanoparticles maintain the globular shape of the parent uncoated nanoparticles, the coating seems to produce some larger aggregates. In Figure 2, some particles, probably constituted by more than one cobalt−ferrite nanoparticle kept together by the silica layer, are indicated by an arrow. This seems to indicate that during the coating procedure some aggregation occurred.[19] As previously said, due to the poor statistic, a TEM evaluation of the magnitude of the aggregation phenomenon due to the coating procedure would be difficult and too expensive in terms of both micrographs acquisition and analysis.

Small Angle Neutron Scattering of Polarized Neutrons. Small angle of polarized neutron scattering can overcome the limits of transmission electron microscopy in the characterization of core−shell magnetic fluids.

In Figure 4 SANSPOL intensities perpendicular to the applied field, I^-(Q⊥H) and I^+(Q⊥H), obtained from un-FF are shown. Both these intensities have been calculated in two separate ways, obtaining identical results: (1) by adjusting the 2-D pattern to the $\sin^2 \alpha$ dependence (see Experimental section) and (2) by averaging the 2-D pattern only over two sectors centered at 90° and 270°, both with a width of 5°.

These spectra have been fitted according to the following equation:

$$I(\mathrm{Q}) = N_\mathrm{p} \int N_\mathrm{p}(\mathrm{R}) V_\mathrm{p}(\mathrm{R})^2 \Delta\rho^2 F(\mathrm{Q,R})^2 \, \mathrm{dR}\, S(\mathrm{Q}) \qquad (7)$$

where N_p and V_p are respectively the number density and the volume of the particles, $\Delta\rho$ is the difference between the scattering length densities of cobalt−ferrite nanoparticles and water, N_p(R) describes the size distribution of the particles, F(Q,R) is their form factor and S(Q) is the structure factor. Considering that the ferrofluid solution is very diluted, we can safely hypothesize that the structure factor S(Q) is equal to 1 and that the SANS curves are determined by the form factor F(Q,R). As suggested by TEM, in the fitting procedure we can

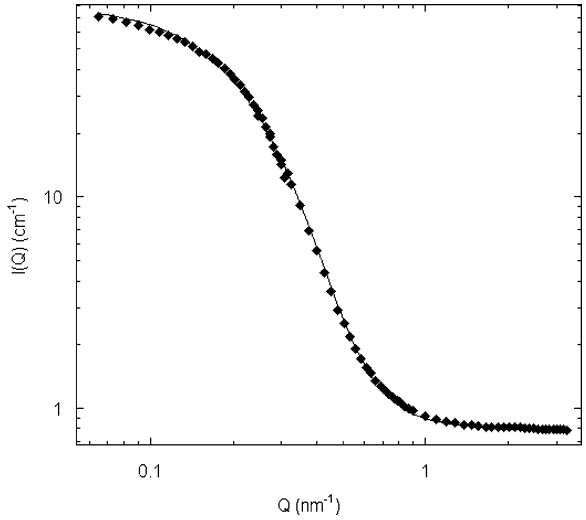

Figure 6. SANSPOL intensities parallel to the applied field I(Q∥H) obtained with un-FF. The solid line represents fitting results according to a spherical model.

use as a guess form the form factor of spherical particles:

$$F_\mathrm{sphere}(\mathrm{Q,R}) = 3[\sin(\mathrm{QR}) - \mathrm{QR}\cos(\mathrm{QR})]/(\mathrm{QR})^3 \qquad (8)$$

We found that this spherical form factor with a Schultz distribution, to take into account polydispersity, can satisfactorily account for the particle shape of the systems investigated.

Results of the fitting routine are shown in Figure 4 as full lines. Both the I^-(Q⊥H) and I^+(Q⊥H) spectra have been fitted at the same time, by constraining all the parameters to be identical for the two spectra, with the exception of the contrast $\Delta\rho$. As said before, $\Delta\rho$ represents the difference between the scattering length densities of cobalt−ferrite nanoparticles and water. Obviously, the scattering length density of water is not dependent on the presence of the magnetic field, while the scattering length density of the nanoparticles is constituted by a nuclear contribution (independent of the magnetic field) and a magnetic contribution. Owing to the inversion of the polarization of the neutrons, the sign of the magnetic contribution is opposite in the I^-(Q⊥H) and I^+(Q⊥H) spectra:

$$\Delta\rho^{(+,-)} = \rho^\mathrm{nucl}_\mathrm{nanoparticles} \pm \rho^\mathrm{mag}_\mathrm{nanoparticles} - \rho_\mathrm{water} \qquad (9)$$

This means that all the fitting parameters have been constrained to be identical for both curves, except for the sign of the magnetic contribution in the previous equation.

Interestingly, after subtraction of the incoherent background, the scattering intensities scale over the whole Q range. This indicates that in the un-FF only magnetic structures are present, i.e., no paramagnetic domains within nanoparticles or iron hydroxide at the surface of the particles are present. In fact, the presence of a layer of $Fe(OH)_3$, due to the modification of the magnetic cross section, would result in a core−shell-like scattering curve, and moreover in a nonscaling behavior of the flipper-on and flipper-off data.

In Figure 5, the size distribution and the volume-weighted size distribution as obtained after the fitting routine are reported. As expected from TEM results, the radius of the nanoparticles ranges from 1 to 15 nm. Moreover, size distributions obtained by TEM and SANSPOL are very similar (see later in this paper).

As in the case perpendicular to the field direction, SANSPOL intensities parallel to the applied field, I^-(Q∥H) and I^+(Q∥H), have been obtained separately by two procedures, obtaining

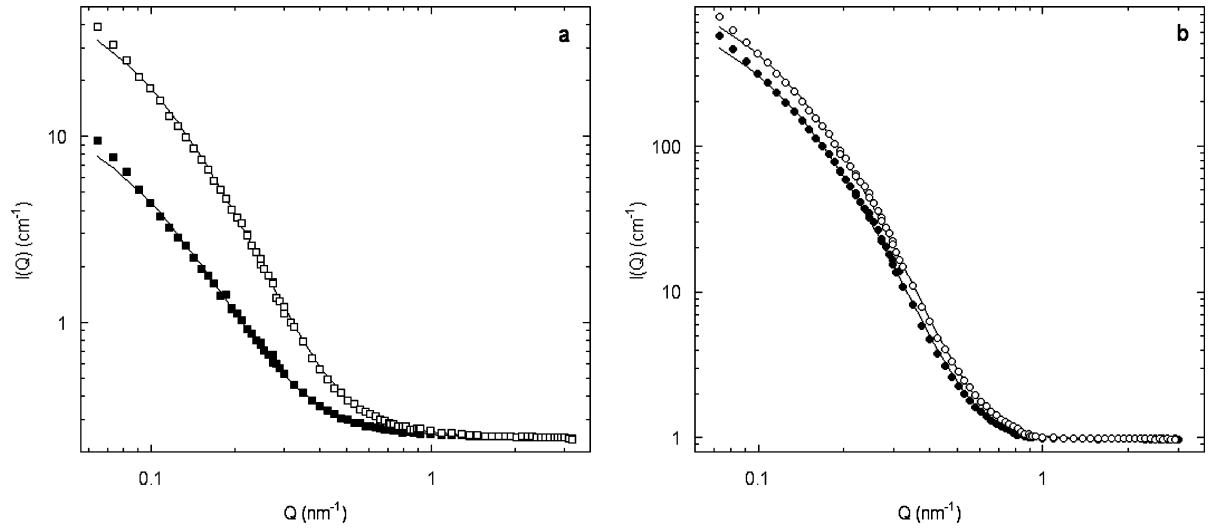

Figure 7. Experimental SANSPOL perpendicular to the applied field data obtained for silica coated cobalt-ferrite nanoparticles. Solid lines: fittings according to a core−shell model. (a) H_2O/D_2O mixture [I^-(Q⊥H) (□), I^+(Q⊥H) (■)]. (b) Pure water [I^-(Q⊥H) (○), I^+(Q⊥H) (●)].

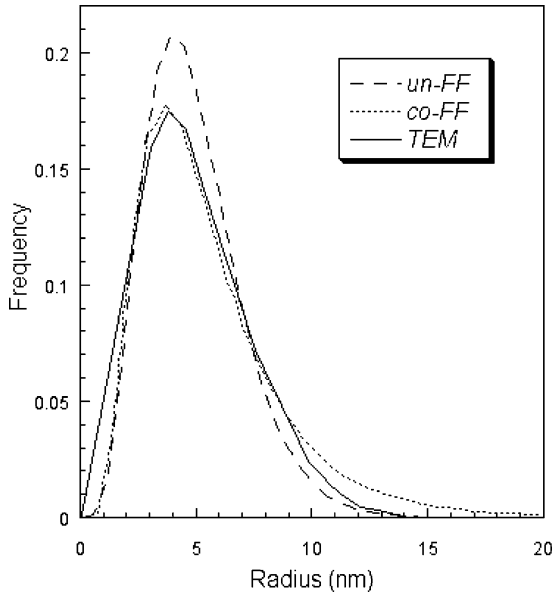

Figure 8. Comparison of size distributions of magnetic nanoparticles as obtained by TEM of un-FF, SANSPOL of un-FF, and SANSPOL of co-FFs (in this latter case size distribution of the core particles is reported).

again identical results: (1) by adjusting the 2-D pattern to the $\sin^2 \alpha$ dependence and (2) by averaging the 2-D pattern over only two sectors centered at 0° and 180°, both with a width of 5°. Moreover I^-(Q∥H) and I^+(Q∥H) are identical within themselves: in fact, as stated in the Experimental section, these intensities account only for the nuclear scattering, being so independent from the applied field and the polarization of neutrons.

In Figure 6 the scattering intensity parallel to the applied field is shown. The full line represents the simulated scattering intensity obtained according to the results of the perpendicular intensity fitting, but imposing the magnetic scattering length density of the nanoparticles $\rho^{\text{mag}}_{\text{nanoparticles}}$ to be equal to zero. The simulated curve is consistent with the data, confirming the goodness of the results obtained by the I(Q⊥H) data fitting.

SANSPOL intensities perpendicular to the applied field obtained from the silica-coated nanoparticles, co-FF, are shown in Figure 7. As previously stated, two co-FFs were prepared: the first one by dispersing the particles in a 30:70 vol. water/heavy water mixture (Figure 7a), and the second one by using pure water (Figure 7b). As in the case of the un-FF, I^-(Q⊥H) and I^+(Q⊥H) were obtained through the $\sin^2 \alpha$ dependence and averaging over small sectors (again, the results are identical). These scattering curves were fitted by using the equation

$$I(\text{Q}) = N_{\text{p}} \int N(R_1) V_{\text{p}}(R_2)^2 F(\text{Q,R})^2 \, \text{dR} \, S(\text{Q}) \qquad (10)$$

where N_{p} and V_{p} are, respectively, the number density and the volume of the particles, R_1 and R_2 are, respectively, the core and shell radii, $N_{\text{p}}(R_1)$ describes the size distribution of the core particles, F(Q,R) is the form factor, and S(Q) is the structure factor. As for the uncoated nanoparticles, we can safely assume S(Q) to be equal to 1. In the fitting procedure we used the typical form factor of core−shell particles:

$$F(\text{Q,R}) = [(\Delta\rho_{\text{core}} - \Delta\rho_{\text{shell}}) F_{\text{sphere}}(\text{Q}R_1) + \Delta\rho_{\text{shell}} F_{\text{sphere}}(\text{Q}R_2)] \qquad (11)$$

Again, the data (in this case four spectra, two for each flipper state) were fitted simultaneously by constraining all the parameters to have the same values within different curves, except for the contrasts:

$$\Delta\rho^{(+,-)}_{\text{core}} = \rho^{\text{nucl}}_{\text{core}} \pm \rho^{\text{mag}}_{\text{core}} - \rho_{\text{solvent}} \qquad (12)$$

$$\Delta\rho_{\text{shell}} = \rho^{\text{nucl}}_{\text{shell}} - \rho_{\text{solvent}} \qquad (13)$$

The size distribution of the magnetic cores obtained at the end of the fitting procedure is reported in Figure 8. For comparison, the size distributions obtained by means of TEM and SANSPOL of the un-FF are shown as well. Results evidence a very good agreement between un-FF results, while the co-FF shows a higher polydispersity, suggesting the formation during the coating procedure of a small number of aggregates constituted by multiple magnetic cores surrounded by the silica layer. This confirms the conclusions from TEM analysis of coated nanoparticles (see Figure 2), where the formation of multiple core nanoparticles was detectable.

With regard to the silica shell, the resulting thickness was 1.8 nm, in good agreement with the 2.0 nm expected from the synthetic pathway we choose.

We then checked if these results were consistent with the SANSPOL intensities parallel to the applied field. As in the

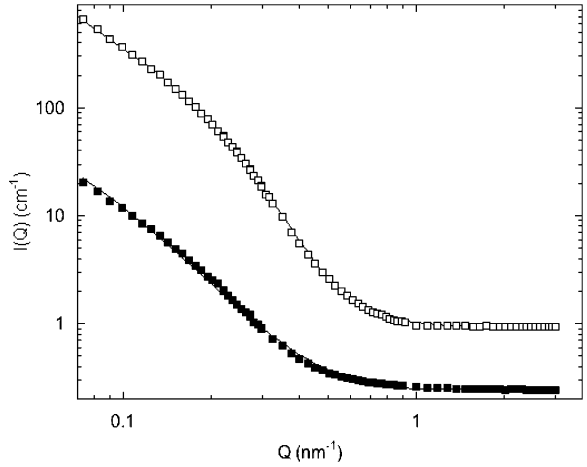

Figure 9. SANSPOL intensities parallel to the applied field $I(Q\|H)$ obtained with co-FF in 30:70 water/heavy water mixture (■) and pure water (□). Solid lines represent the fittings according to the results obtained by the perpendicular to the field data, assuming $\rho_{core}^{mag} = 0$.

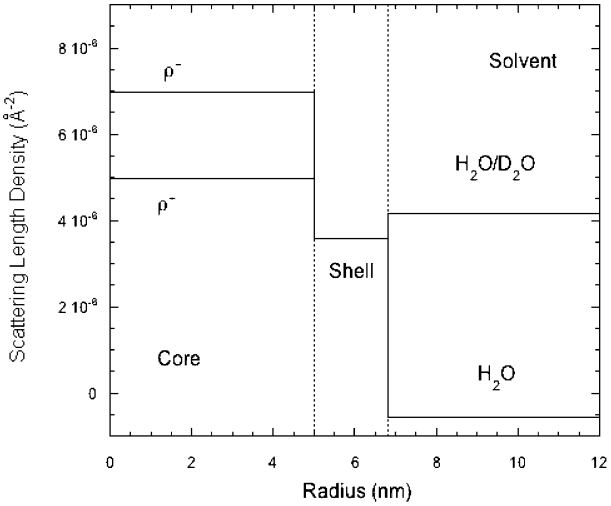

Figure 10. Schematic scattering length density profile as obtained from SANSPOL intensity fitting procedure.

case of the un-FF, $I^-(Q\|H)$ and $I^+(Q\|H)$ were obtained by the same two procedures, obtaining again identical results, in terms of both procedures and polarizations. In Figure 9 the scattering intensities parallel to the applied field are shown. The full lines represent the simulated scattering intensities obtained according to the results of the perpendicular intensity fitting, but imposing the magnetic scattering length density of the nanoparticles ρ_{core}^{mag} in eq 12 to be equal to zero. The simulated curves are consistent with the data, confirming the results obtained through the $I(Q\perp H)$ data fitting.

The scattering length density profile, as obtained by theoretical evaluation (nuclear scattering length densities) and SANSPOL data fitting procedure (magnetic scattering length density), is shown in Figure 10.

Conclusions

This work reports the synthesis of silica-coated cobalt−ferrite nanoparticles in water and their characterization by means of SANSPOL analysis. We demonstrated how SANSPOL, recently developed, constitutes a powerful tool for the investigation of ferrofluids. In particular, we showed how TEM studies of core−shell nanoparticles sometimes are not sufficient to provide a full and detailed picture of magnetic fluids. SANSPOL is very powerful since it takes advantage of the modification of the magnetic cross section produced in a spin flipper experiment using polarized neutrons. This experiment allows determination of both magnetic and diamagnetic domains that could be present in nanoparticles

Using SANSPOL analysis we found that core−shell cobalt−ferrite nanoparticles present a uniform silica shell that can be obtained by a very simple synthetic procedure. The thickness of this coating does not depend on the size of the cobalt-ferrite particles and it does not change the shape of the coated particle.

Acknowledgment. The Italian Ministry for Scientific Research (MIUR grant PRIN2003), European Union (grant HPRI-CT-2001-00138), and CSGI are acknowledged for financial support.

References and Notes

(1) Papell, S. S. U.S. Patent 3,215,572, 1965.

(2) Berkovsky, B.; Bashtovoy, V. *Magnetic Fluids and Applications Handbook*; Begell House Inc.: New York, 1996.

(3) Petit, C.; Taleb, A.; Pileni, M. P. *J. Phys. Chem. B* **1999**, *103*, 1805−1810.

(4) Bonini, M.; Bardi, U.; Berti, D.; Neto, C.; Baglioni, P. *J. Phys. Chem. B* **2002**, *106*, 6178−6183.

(5) Sangregorio, C.; Galeotti, M.; Bardi, U.; Baglioni, P. *Langmuir* **1996**, *12*, 5800−5802.

(6) Massart, R.; U.S. Patent 4,329,241, 1982.

(7) Massart, R.; Dubois, E.; Cabuil, V.; Hasmonay, E. *J. Magnetism Magnetic Mater.* **1995**, *149*, 1−5.

(8) Morais, P. C.; Garg, V. K.; Oliveira, A. C.; Silva, L. P.; Azevedo, R. B.; Silva, A. M. L.; Lima, E. C. D. *J. Magnetism Magnetic Mater.* **2001**, *225*, 37−40.

(9) Donselaar, L. N.; Philipse, A. P.; Suurmond, J. *Langmuir* **1997**, *13*, 6018−6025.

(10) Correa-Duarte, M. A.; Giersig, M.; Kotov, N. A.; Liz-Marzan, L. M. *Langmuir* **1998**, *14*, 6430−6435.

(11) Butterworth, M. D.; Illum, L.; Davis, S. S. *Colloids Surf., A* **2001**, *179*, 93−102.

(12) Santra, S.; Tapec, R.; Theodoropoulou, N.; Dobson, J.; Hebard, A.; Tan, W. *Langmuir* **2001**, *17*, 2900−2906.

(13) Qhobosheane, M.; Santra, S.; Zhang, P.; Tan, W. H. *Analyst* **2001**, *126*, 1274−1278.

(14) Moon, R. M.; Riste, T.; Koehler, W. C. *Phys. Rev.* **1969**, *181*, 920−931.

(15) Keller, T.; Krist, T.; Danzig, A.; Keiderling, U.; Mezei, F.; Wiedenmann, A. *Nucl. Instrum. Methods Phys. Res., Sect. A* **2000**, *451*, 474−479.

(16) Wiedenmann, A. *J. Appl. Crystallogr.* **2000**, *33*, 428−432.

(17) Wiedenmann, A. In *Lecture Notes in Physics*; Odenbach, S., Ed.; Springer: Berlin, 2002; pp 33−61.

(18) Heinemann, A.; Wiedenmann, A. *J. Appl. Crystallogr.* **2003**, *36*, 845−849.

(19) Lu, Y.; Yin, Y. D.; Mayers, B. T.; Xia, Y. N. *Nano Lett.* **2002**, *2*, 183−186.

(20) Wiedenmann, A. *Physica B* **2001**, *297*, 226−233.

(21) Neveuprin, S.; Tourinho, F. A.; Bacri, J. C.; Perzynski, R. *Colloids Surf/. A* **1993**, *80*, 1−10.

(22) Zins, D.; Cabuil, V.; Massart, R. *J. Mol. Liq.* **1999**, *83*, 217−232.

(23) Sousa, M. H.; Tourinho, F. A.; Depeyrot, J.; da Silva, A. F.; Lara, M. C. L. *J. Phys. Chem. B* **2001**, *105*.